

Unique Simulation Technique to Predict Accelerations and Frequencies at Different Locations of Human Body and Seat Inside an Accelerating Car

Purnendu Mondal¹

¹PMS SOLUTIONS LTD, FLAT 4, 24 Hartington Street, Derby, UK-DE23 8EA

Abstract— Measuring the levels of vibration inside the human body and its sitting medium is one of the primary means of monitoring the health and safety of in-vehicle human. In this research paper, a unique finite element based simulation methodology has been proposed to predict the levels of vibration at different locations of human driver and seat inside a moving car. This technique aims to replace the costly and time consuming testing method to measure vibration. A non-robust car seated human model has been established and vertical accelerations with respect to time for human and seat segments have been extracted from simulation. Frequencies of human and seat portions have been evaluated and compared to data from past research works. Representation of human segments through ellipsoidal elements, assignment of shape specific three dimensional stiffness parameters and prediction of final vibration data inside entire human-car seat system, make this methodology unique in nature.

Keywords— Ellipsoidal human segment, Finite element, Frequency Human biodynamics, Simulation, Three dimensional stiffness parameters, Vertical acceleration, Vibration.

I. INTRODUCTION

Computerized simulation methodologies for assessing, measuring and monitoring level of vibration inside the human-automotive system have been developed over last few decades. The sitting posture, seat orientation and contact mechanism between the human body and automotive seat are the most crucial factors for the biodynamic vibration analysis of the in-vehicle seated human body. The posture of a seated human body inside any automotive must be in accordance with the relevant industrial standards. ISO/TC 159/SC 1, ISO/TC 159/SC 3, ISO/TC 159/SC 4 and ISO/TC 159/SC 5 provide the guidelines for the anthropometry, bio-mechanics, human interface ergonomics and environmental ergonomics, respectively.

Study on the entire vehicle dynamics using simulation method [1] stated that the computer based technologies for analyzing automotive dynamics are becoming advantageous cause of the high cost associated to the practical vehicle development process. One dimensional tool Modelica and three dimensional finite element tool were used [2] to simulate the riding comfort of human body, where the whole body was divided into fourteen segments. Contact mechanisms had been assigned in-between the mating surfaces and the level of vibration excitement was evaluated. Finite element based study for the vibration transmissibility between the human and automotive [3] considered torso, pelvis, thigh, leg, feet, neck, head, arm and hand along with the muscle properties. The outcome of that study was able to anticipate the vibration transmissions into the human spine in the fore-aft and vertical directions. Similar kind of finite element work on vibration transmissibility between the human and automotive seat [4] examined several human bodies under the effect of vertical vibration. All the portions of the human body were modelled in finite element environment, where the average mass and

height of the experimental human bodies were 68.5 kg and 174 cm, respectively.

A finite element model of automotive seat was established [5] using polyurethane foam and springs to analyze the vibration in vertical direction. Three dimensional analysis of seated human body using LS Dyna was conducted [6] to assess the contact behaviour at the mating interfaces between the human body and automotive seat. Vibration transmission from the human occupant to seat backrest was analyzed [7] numerically using multi-point input method, which concluded that the levels of vibration at the corners of seat cushion would highly be dependent on the acceleration of seat backrest. Both the finite element and multi-body tools were used [8] to construct an aviation mode seat utilizing shell, beam and joint elements for understanding the effect of acceleration.

Sitting process of the driver inside an automotive was simulated in RAMSIS [9] to analyze the human comfort with the concept of non-movable eye, hip, hand and heel. The results from that study optimized the comfortable orientations of various human portions.

Modelling the appropriate properties of the foam material for the automotive seat is necessary to analyze the dynamic interaction between the seat and human body effectively. Non-linear nature and hysteresis response of the seat foam material under the effect of repetitive loading conditions were shown in the study of car seat using finite element method [10]. Dynamic crash simulation of polymeric foam excited with uniaxial compression [11] showed the stress-strain behaviour of foam material in graphical format, while finite element study on the properties of car seat foam polyurethane material [10] reported that the relationship between stress and strain inside the foam material would be a function of the strain rate.

After reviewing the earlier research works carried out on the automotive-human system, it is obviously clear that most of the past investigations were focused mainly on the very specific portions of the whole human-seat assembly. Few

studies considered the entire human occupant and automotive seat, though the assessments from those studies were limited to the vibration transmission, mode shape related frequency or contact interface between the mating surfaces. Moreover, most of the past investigations considered the stiffness parameters of the human segments from the standard database or handbook, therefore ignored the human size specific stiffness values.

In the current research work, a finite element simulation based model of car-seated human driver has been constructed as per the real life driving posture and seat orientation. Material properties of the human bone and muscle have been combined together and anthropometric data have been consulted to evaluate the three dimensional size specific stiffness values for human portions. Hyperelastic and viscoelastic material properties have been assigned to the car seat foam and suitable contact mechanisms have been implemented at the mating surfaces in between the human body and car seat. Boundary and load conditions have been applied as per the real life driving conditions. Displacements and accelerations in the vertical direction have been extracted from the results and frequency magnitudes at various points of human body and car seat have been evaluated. The obtained frequencies have been compared to the outcomes of similar past research works, while the vertical accelerations have been compared to the practical testing data obtained from similar operating environment. The outlined unique finite element simulation methodology is successful in anticipating the levels of vibration at different locations of human body and seat inside a moving car.

II. SIMULATION METHODOLOGY

A. Masses and Dimensions of Human Segments

A 50th percentile male human model of 77.3 kg mass has been taken into account for setting up the simulation. The masses of the human portions have been calculated following the guidelines provided in the databases of human segmental parameters [12], [13]. Basic instructions for measuring the dimensions of the human body parts have been outlined in the international standards PD ISO/TR 7250-2:2010 and BS EN ISO 7250:1998. A comprehensive data set of anthropometric dimensions has been shown [14] based on the principal component analysis, while the essential factors for human comfort have been published in the handbook of human ergonomics [15]. After careful consultation with all the relevant literatures, standards and handbooks, human segmental dimensions have been gathered to set up the human model in simulation environment.

B. Human portions represented by ellipsoidal bodies

To carry out an effective simulation of the whole human body and automotive seat assembly, it is advantageous to simplify the human model prior to taking it into the simulation environment. One of the most effective ways to simplify the complex human body is to represent the human portions by ellipsoidal segments. Academic study on the eigen vectors of human portions [16] represented the human segments by truncated ellipsoids, axes lengths of which were taken from

the anthropometric database. Study on the deformations of the human leg and arm [17] explained the displacement phenomenon of a point on ellipsoidal cross-section to understand the benefit of representing human segments by ellipsoids.

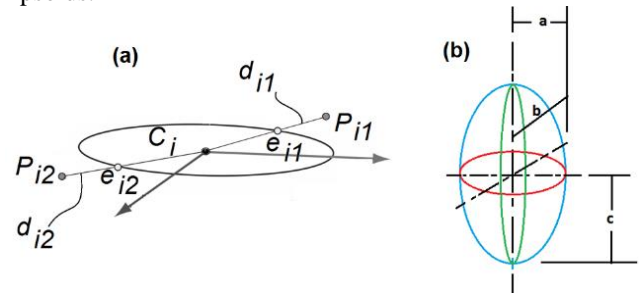


Figure 1: (a) Displaced point on ellipsoidal cross-section and (b) half lengths along axial directions of ellipsoid

The deviation of a displaced point on ellipsoidal section from its original location is shown in Figure 1 and can be derived from the Equation 1.

$$D(u_{ij}, v_i) = d_{ij} = \|P_{ij} - e_{ij}\| \quad (1)$$

$$i = 1, \dots, M,$$

$$j = 1, \dots, N_i$$

(u_{ij}, v_i) = Surface parameters of the point e_{ij} on ellipsoidal surface C_i .

Head, torso, upper arms, lower arms, hands, thighs, legs and feet of the human body have been modelled as ellipsoidal bodies, the axes lengths of which are based on the collected anthropometric data. Later, ratios of lateral axes, average volume and density of each of the ellipsoidal segments have been calculated.

One of the most effective ways to simplify the complex human body structure is to represent the human portions by ellipsoidal segment. Academic study on the eigen vectors of human portions considered [16] the truncated ellipsoids and the axes lengths were extracted from anthropometric database. Deformation study on the human leg and arm [17] gave an idea of representing human portion by ellipsoidal cross-section.

C. Driving posture of Human

The comfortable orientations of the car seated human portions can be assigned based on the guidelines provided in global standards ISO/TC 159/SC 1, ISO/TC 159/SC 3 and ISO/TC 159/SC 4 for ergonomic principles, anthropometric informations and system-human bio-mechanic interaction, respectively.

To make this simulation practical, photograph of a car seated male human driver of 77 kg mass has been imported into Solidworks 2019 drafting environment and all the angular dimensions of different portions have been measured. Based on these measured orientations of different body portions, a parametric three dimensional assembly of car seated human driver has been constructed and seating posture has been assigned. The photograph with angular dimensions and established assembly are shown in Figure 2.

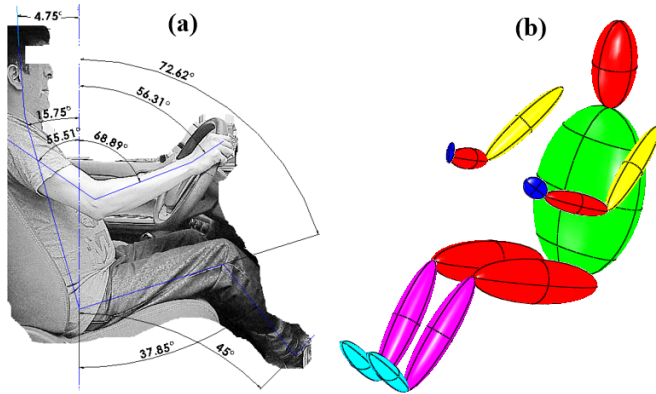


Figure 2: (a) Real human male driver sitting on a car seat and (b) constructed CAD assembly of driver human

D. Properties of Human Body Segments in Simulation Environment

Mechanical properties of human bone and muscle are complex and non-linear in nature. Skins and muscles exhibit the combination of hyper-elastic and viscoelastic material properties and as a result, finding the accurate value of Young's Modulus (YM) of the integrated structure of human bone and soft tissue is a challenging task. While exploring the properties of bones for the human bodies of different gender and age [16], the YM value of the human bone was found as 20.04 GPa. Similar investigation using finite element tool considered [18] the YM of human bone as 15 GPa. Indentation test and tensile strength measurement of the biological tissue found the YM values for muscles and tissues in the range of 3 kPa - 8 kPa. In the current research study, YM values for human muscles and bones have been taken as 8 kPa and 20.04 GPa, respectively.

Depending on the aspects of the bio-dynamic research work, the human bone-muscle integrated structure can be represented either through fibre, composite or silicon based substances. Composite materials have got distinct advantage over all other materials as the three directional stiffness parameters inside the composite body can be calculated using dedicated formulations. For all the human segments in the present simulation study, the percentages of muscles and bones have been considered as 85% and 15%, respectively as defined in the advanced human nutrition database [19] Later, using the formulations of Equation 2 and Equation 3, three dimensional YM values for each of the human portions have been evaluated.

$$E_{i-Axial} = E_{Muscle} \times f_{Muscle} + E_{Bone} \times (1 - f_{Muscle}) \quad (2)$$

$$E_{i-Transverse} = \frac{E_{Muscle} \times E_{Bone}}{E_{Muscle} \times (1 - f_{Muscle}) + E_{Bone} \times f_{Muscle}} \quad (3)$$

$E_{i-Axial}$ = Axial YM of i^{th} segment

$E_{i-Transverse}$ = Transverse YM of i^{th} segment

Combining the gathered dimensions and calculated YM values, three directional stiffness values for all the human portions have been calculated using the mathematical formulation of Equation 4 co-relating the force, stress, strain and cross-sectional area.

$$K_{ij-Directional} = \pi \frac{E_{ij-Directional} a_{per-ij-Directional} b_{per-ij-Directional}}{C_{ij-Directional}} \quad (4)$$

$K_{ij-Directional}$ = Stiffness of j^{th} segment in i^{th} direction

$E_{ij-Directional}$ = YM of j^{th} segment in i^{th} direction

$a_{per-ij-Directional}$ = Half axis (Transverse axis-1) length of the of j^{th} segment perpendicular to i^{th} direction

$b_{per-ij-Directional}$ = Half axis (Transverse axis-2) length of the of j^{th} segment perpendicular to i^{th} direction

$C_{ij-Directional}$ = Half axis length of the of j^{th} segment in i^{th} direction

Human muscles are made of soft tissues, which are incompressible in nature. Poisson's ratio for incompressible materials falls in the range of 0.45 to 0.49. Finite element study on human muscles [20] considered Poisson's ratio as 0.49995, while measurement of YM value for soft human tissue [21] considered the Poisson's ratio as 0.49. Human bones are ideally constructed by rigid materials and most of the past research works used the rigid material properties to model the human bone elements. Practically, the soft and non-rigid human muscles are more viable to be deformed quicker than the rigid bones, hence, for this simulation methodology the Poisson's ratio has been assigned as 0.49.

Besides the YM, stiffness value and Poisson's ratio, it is necessary to define the damping parameters for the human segments. The empirical expression to define a damped system can be described as shown in Equation 5.

$$[C] = \alpha[M] + \beta[K] + \sum_{j=1}^{N_{mat}} \beta_j [K_j] + \beta_c [K] + [C_\zeta] + \sum_{k=1}^{N_{el}} [C_k] \quad (5)$$

α = Mass matrix multiplier constant

β = Stiffness matrix multiplier constant

β_j = Material dependent stiffness matrix multiplier constant

β_c = Variable stiffness matrix multiplier constant

C_ζ = Frequency dependent damping matrix

C_k = Element damping matrix

j = Material (1, ..., N_{mat})

k = Element (1, ..., N_{el})

This finite element based simulation study primarily focuses on the frequency dominated results. So, attention has been paid to the frequency dependent damping matrix of the system, which can be expressed through Equation 6 as a function of the mode shapes.

$$\{u_r\}^T [C_\zeta] \{u_r\} = 4\pi f_r \zeta_r \quad (6)$$

u_r = r^{th} mode shape

f_r = Frequency at r^{th} mode shape

ζ_r = Damping ratio for r^{th} mode shape

ζ can further be explained through Equation 7.

$$\zeta_r = \zeta + \zeta_{mr} \quad (7)$$

ζ = Constant damping ratio

ζ_{mr} = Modal damping ratio for r^{th} mode shape

Damping coefficients for the head, back, torso, thorax and abdomen had been considered as 3575.506 Ns/m, 3575.506 Ns/m, 3575.506 Ns/m, 291.878 Ns/m and 291.878 Ns/m, respectively during the investigation of a seated human of 80 kg mass [22]. Study on the vertical and fore-aft vibrations inside a human body of 75 kg mass [23] considered the damping coefficients as 2376.4 Ns/m, 145.8 Ns/m, 1797.7 Ns/m and 1797.7 Ns/m for lower torso, arms, upper torso and hands, respectively. Analysis of human body of 90 kg mass [24] assumed the damping coefficients for head-neck, chest-upper torso, lower torso and pelvis-thigh to be 620 Ns/m, 8550 Ns/m, 5685 Ns/m and 3564 Ns/m, respectively.

The damping co-efficients for the human portions in this simulation work have been chosen from the past investigations with the closest match in terms of human mass. For head, torso, upper arms, lower arms, hands, thighs, legs and feet, the damping coefficients have been selected as 620 Ns/m, 1797.7 Ns/m, 145.8 Ns/m, 145.8 Ns/m, 1797.7 Ns/m, 2376.4 Ns/m, 2376.4 Ns/m and 2376.4 Ns/m, respectively. Constant damping ratio has been assigned with a value of 0.2 as directed by the analyses of human joints [25], [26].

E. Car Seat Modelling and Material Properties in Simulation Environment

Design of car seats and relevant processes had been modified over last many years based on the ergonomics and industrial aspects. From the database of one of the pioneer seat design houses named “Ricaró”, an idea of the evolution of car seats over last half century can be obtained. Specification on the human fitness parameters [27] suggested the least width of seat cushion to be 432 mm for 95th percentile female human body, though bigger size would be advantageous considering the clothing. Study on seat parameters [28] suggested the minimum width of seat cushion to be in the range of 480 mm to 500 mm. Length of the seat cushion had been recommended as 432 mm [29] and 440 mm to 550 mm [28]. Survey of seat design recommended the minimum width and height of backrest to be 360 mm and 410 mm to 550 mm above H-point, respectively. After consulting with relevant recommendations and databases, a computer aided model of car seat has been constructed. Metallic frames and other associated structures of the car seat have been ignored.

As the modern industries are inclined more towards the foam type seats over mechanical suspension type, a polyurethane foam type car seat has been used during this simulation study. Polyurethane material can be modelled by using the hyper-elastic, combined hyper-elastic and visco-elastic or stress-strain formulation.

Following the international standard ASTM D 3574 – 01 for test methods of flexible cellular materials, co-relation between the strain and stress inside foam material had been evaluated [30]. During that study, the strain energy absorption capacity of the hyper-elastic material was described through the formulation of Ogden model as presented in Equation 8.

$$[U] = \sum_{i=1}^N 2 \frac{\mu_i}{\alpha_i^2} [\tilde{\lambda}_1^{\alpha_i} + \tilde{\lambda}_2^{\alpha_i} + \tilde{\lambda}_3^{\alpha_i} - 3 + \frac{1}{\beta_i} ((J^{el})^{-\alpha_i \beta_i} - 1)] \quad (8)$$

N = Defining parameter for the approximation of the model

$\tilde{\lambda}_j$ = Principal strength j

J^{el} = Elastic volumetric ratio

α_i, β_i, μ_i = Material dependent parameters

Later, the outputs from the test set up were exported to finite element environment and Ogden hyper-elastic coefficients had been evaluated using the curve fitting technique. The coefficient values of the strain energy potential function obtained from that investigation were $\mu_1 = 164.861$ kPa, $\alpha_1 = 8.88413$, $\beta_1 = 0.0$, $\mu_2 = 0.023017$ kPa, $\alpha_2 = 4.81798$, $\beta_2 = 0.0$. Similar kinds of mathematical models had been offered for the performance studies of slightly compressible hyper-elastic materials [31] and highly compressible hyper-elastic materials [32]. Finite element based modelling of the hyper-elastic foam material [33] optimized the Ogden parameter values for finite element applications. The optimized Ogden coefficient (N=2) values were $\mu_1 = 0.00481$ MPa, $\alpha_1 = 19.8$, $\beta_1 = 0.01450$, $\mu_2 = 0.00360$ MPa, $\alpha_2 = 19.8$, $\beta_2 = 0.00650$. In the present simulation study, hyper-elastic properties have been assigned to the seat foam material using these optimized Ogden coefficient (N=2) values.

Modelling of automotive seat [10] found the density of the foam material as 67 kg/ m³. Assessment of different kinds of polyurethane foams [34] reported a comprehensive database of foam densities with respect to variable cell sizes. Thesis on auxetic polyurethane foam [35], study on automotive comfort [36], modelling of visco-elastic material [37] and investigation of the Poisson’s ratio of seat foam material [38] used the densities of polyurethane material as 27 kg/ m³, 37-52 kg/ m³, 28 kg/ m³ and 32-64 kg/ m³ respectively. In the current simulation work, the density value of the polyurethane foam has been used as 64 kg/ m³.

Practically, the seat foam material deforms mostly under the effect of compression in absence of any sidewise constraint and as a result, no direct relationship can be established between the lateral strain and longitudinal strain. Considering this fact, the computational analysis method of the car seat [30] assumed the Poisson’s ratio as 0. Finite element based modelling of the automotive seat [10] ignored the Poisson’s ratio, too. Poisson’s ratio has been ignored during this course of simulation work.

F. Car Seat Modelling and Material Properties in Simulation Environment

Design of car seats and relevant processes had been modified over last many years based on the ergonomics and industrial aspects. From the database of one of the pioneer seat design houses named “Ricaró”, an idea of the evolution of car seats over last half century can be obtained. Specification on the human fitness parameters [27] suggested the least width of seat cushion to be 432 mm for 95th percentile female human body, though bigger size would be advantageous considering the clothing. Study on seat parameters [28] suggested the minimum width of seat cushion to be in the range of 480 mm to 500 mm. Length of the seat cushion had been recommended as 432 mm [29] and 440 mm to 550 mm [28]. Survey of seat design recommended the minimum width and height of backrest to be 360 mm and 410 mm to 550 mm above H-point,

respectively. After consulting with relevant recommendations and databases, a computer aided model of car seat has been constructed. Metallic frames and other associated structures of the car seat have been ignored.

As the modern industries are inclined more towards the foam type seats over mechanical suspension type, a polyurethane foam type car seat has been used during this simulation study. Polyurethane material can be modelled by using the hyper-elastic, combined hyper-elastic and visco-elastic or stress-strain formulation.

Following the international standard ASTM D 3574 – 01 for test methods of flexible cellular materials, co-relation between the strain and stress inside foam material had been evaluated [30]. During that study, the strain energy absorption capacity of the hyper-elastic material was described through the formulation of Ogden model as presented in Equation 8.

$$[U] = \sum_{i=1}^N 2 \frac{\mu_i}{\alpha_i^2} [\tilde{\lambda}_1^{\alpha_i} + \tilde{\lambda}_2^{\alpha_i} + \tilde{\lambda}_3^{\alpha_i} - 3 + \frac{1}{\beta_i} ((J^{el})^{-\alpha_i \beta_i} - 1)] \quad (8)$$

N = Defining parameter for the approximation of the model

$\tilde{\lambda}_j$ = Principal strength j

J^{el} = Elastic volumetric ratio

α_i, β_i, μ_i = Material dependent parameters

Later, the outputs from the test set up were exported to finite element environment and Ogden hyper-elastic coefficients had been evaluated using the curve fitting technique. The coefficient values of the strain energy potential function obtained from that investigation were $\mu_1 = 164.861$ kPa, $\alpha_1 = 8.88413$, $\beta_1 = 0.0$, $\mu_2 = 0.023017$ kPa, $\alpha_2 = 4.81798$, $\beta_2 = 0.0$. Similar kinds of mathematical models had been offered for the performance studies of slightly compressible hyper-elastic materials [31] and highly compressible hyper-elastic materials [32]. Finite element based modelling of the hyper-elastic foam material [33] optimized the Ogden parameter values for finite element applications. The optimized Ogden coefficient ($N=2$) values were $\mu_1 = 0.00481$ MPa, $\alpha_1 = 19.8$, $\beta_1 = 0.01450$, $\mu_2 = 0.00360$ MPa, $\alpha_2 = 19.8$, $\beta_2 = 0.00650$. In the present simulation study, hyper-elastic properties have been assigned to the seat foam material using these optimized Ogden coefficient ($N=2$) values.

Modelling of automotive seat [10] found the density of the foam material as 67 kg/ m³. Assessment of different kinds of polyurethane foams [34] reported a comprehensive database of foam densities with respect to variable cell sizes. Thesis on auxetic polyurethane foam [35], study on automotive comfort [36], modelling of visco-elastic material [37] and investigation of the Poisson's ratio of seat foam material [38] used the densities of polyurethane material as 27 kg/ m³, 37-52 kg/ m³, 28 kg/ m³ and 32-64 kg/ m³ respectively. In the current simulation work, the density value of the polyurethane foam has been used as 64 kg/ m³.

Practically, the seat foam material deforms mostly under the effect of compression in absence of any sidewise constraint and as a result, no direct relationship can be established between the lateral strain and longitudinal strain. Considering this fact, the computational analysis method of the car seat [30] assumed the Poisson's ratio as 0. Finite

element based modelling of the automotive seat [10] ignored the Poisson's ratio, too. Poisson's ratio has been ignored during this course of simulation work.

G. Simulation Set Up- Assembly, Boundary Condition, Interaction, Meshing and Load Case

The modelled human body and car seat have been assembled avoiding any interference and maintaining closest possible proximity. Later the full assembly has been imported into finite element tool ABAQUS CAE 6.13. The boundary conditions have been applied as practical as possible. The head is restrained to be in touch with the headrest, but sidewise movement is allowed. Rotation of the hands about the steering wheel is permitted, but detachment from the steering wheel is restricted. Angular orientations of the feet about the ankle connections are acceptable, but separations from the clutch and brake positions are restricted. All the adjacent human segments are connected through tie-up constrains as shown with lines in Figure 3. Bottom surface of the seat cushion is fixed, angular fore-aft movement of the backrest about the seat pivot point is permitted, sidewise movement of the backrest backend is restricted, angular fore-aft orientation of headrest about the connecting point to the backrest is allowed and sidewise movement of the headrest backend is restricted.

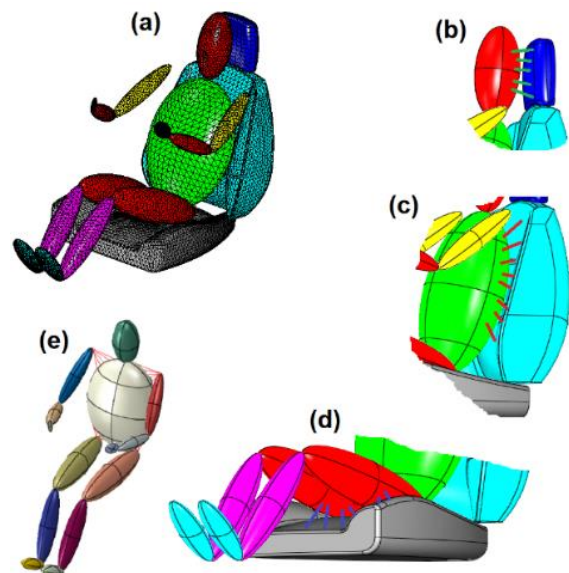


Figure 3: (a) Meshed assembly (b) tie constraint between human head and seat headrest and (c) tie constraint between human torso and seat backrest (d) tie constraint between human thighs and seat cushion (e) tie constraint between human portions

In the next stage of simulation set up, contact mechanisms at the mating surfaces between human body and car seat have been assigned. Most of the past automotive contact related research works investigated mainly the pressure distribution, stress level or vibration transmission by taking into account the portions of human body and seat. From the outcomes of the studies on comfortable human orientation [30] [39] [40], pressure at the human-seat interface [41] [42], seat cushion with human buttock [43] and human sitting process [9], it is inevitably clear that all the past automotive-human interaction

related investigations tried to minimize the number of mating surfaces to reduce the complexity inside simulation. After careful judgment of pros and cons of different contact mechanisms, multi-point constraint (MPC) formulation has been assigned in-between the human body and car seat in this simulation work. MPC ties the movements of contacting surfaces together and supports large deformations in the simulation system.

Ten-node tetrahedral element - C3D10 has been used for generating meshes inside human body and car seat.

Linear perturbation and modal dynamic steps have been implemented to run the analysis. Figure 3 displays the driver-seat meshed assembly and the tie constraints between the human body and car seat.

Load scenario in this simulation is based on a non-racer type accelerating car picking up speed of 30 miles/hr from static condition on smooth road terrain. Hence, the load has been assumed to be appearing primarily from the effect of startup acceleration. Acceleration values of non-racer automobile at 60 km/hr and 40 km/hr [44] had been reported to be 1.083 m/sec² and 0.861 m/sec², respectively. Average and maximum acceleration values for the passenger vehicle operating in rural area were predicted using the Equation 9 and Equation 10 [45].

$$a_{av} = ae^{bv} \tag{9}$$

$$a_{max} = c + dv \tag{10}$$

a_{av} = Average acceleration in m/sec²

a_{max} = Maximum acceleration in m/sec²

v = Vehicle speed in m/sec

a, b, c, d = Constants

Considering the closest match in terms of the nature of the vehicle operating environment, the acceleration value of 0.861 m/sec² has been considered in the current simulation study. Loading scenario has been made to be effective in the modal dynamic step after obtaining eigen frequencies from the linear perturbation step. Modal dynamics step takes into account the damping of the system and constructs the system matrix based on the mode shapes received from previous step.

III. RESULTS FROM THE SIMULATION

A 64 bit computer with Windows XP operating system, 6 GB of RAM and two dual-core 2.1 GHz Intel(R) Pentium(R) CPU B950 processors has been used to run the simulation. Cause of the hardware limitation, the simulation running time was set to 10 seconds and ABAQUS solver took around 11 wall-clock hours to complete the analysis.

Finding the responses of the human body and car seat portions under the effect of vertical vibration is the primary aim of this simulation study. Hence, vertical accelerations and displacements at head, upper arm, lower arm, chest, waist, thigh, legs, cushion, headrest and backrest have been extracted from the ABAQUS post processor. The points of interest for extracting the vertical accelerations are shown in Figure 4.

Figure 5, Figure 6, Figure 7, Figure 8, Figure 9, Figure 10, Figure 11, Figure 12, Figure 13 and Figure 14 are showing the vertical acceleration values with respect to time for all the human body and car seat portions.

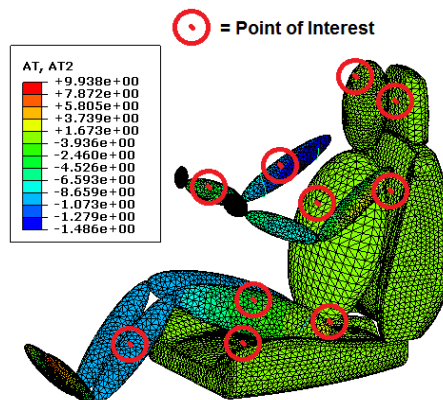


Figure 4: Points of interest and vertical acceleration

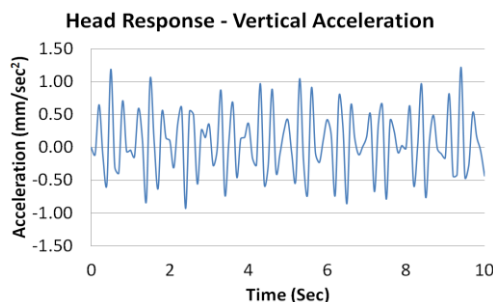


Figure 5: Vertical acceleration at head

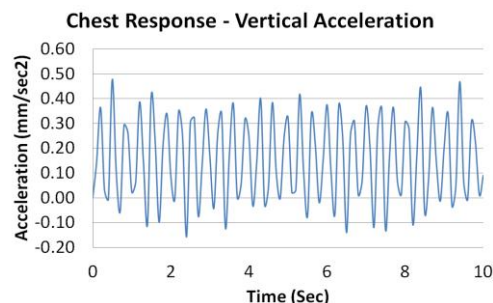


Figure 6: Vertical acceleration at chest

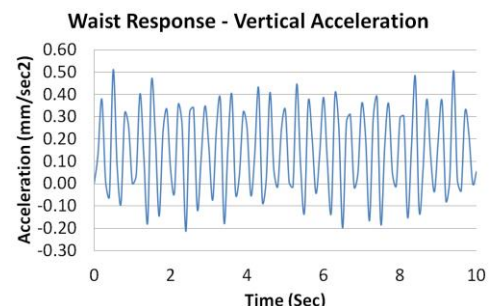


Figure 7: Vertical acceleration at waist

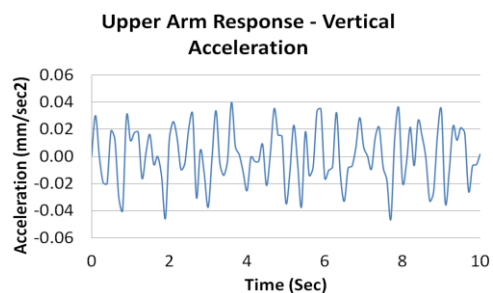


Figure 8: Vertical acceleration at upper arm

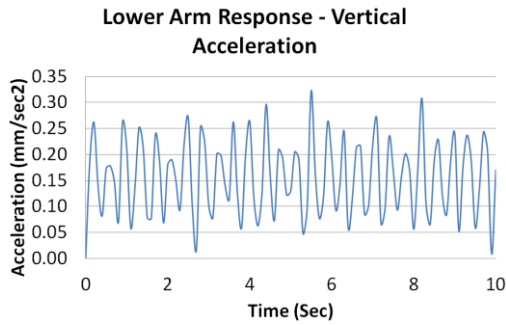


Figure 9: Vertical acceleration at lower arm

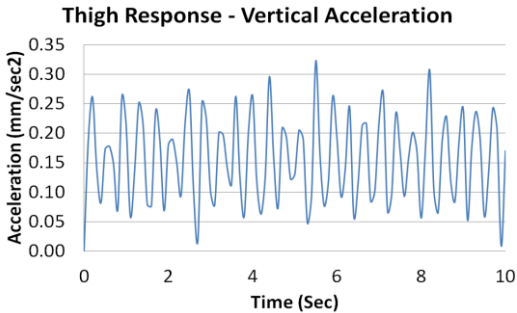


Figure 10: Vertical acceleration at thigh

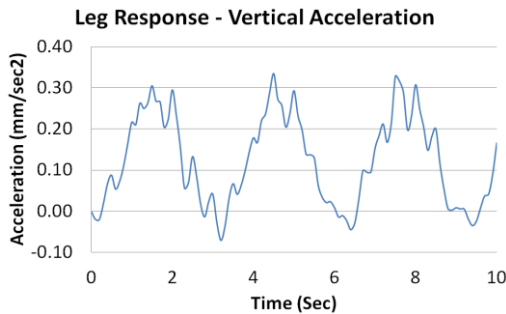


Figure 11: Vertical acceleration at leg

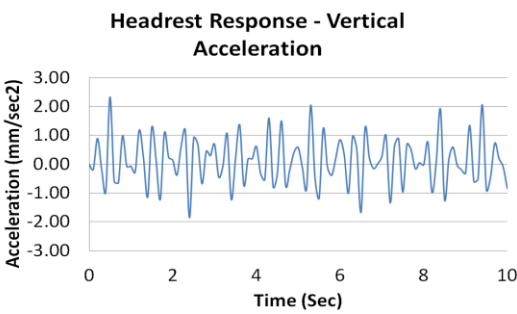


Figure 12: Vertical acceleration at headrest

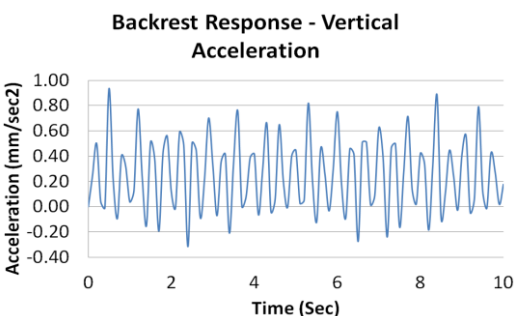


Figure 13: Vertical acceleration at backrest

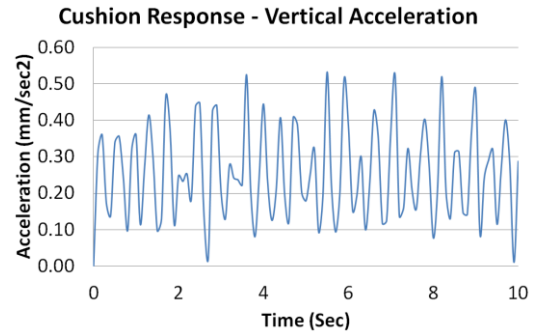


Figure 14: Vertical acceleration at cushion

Vertical displacement values with respect to time for all the human body and car seat portions are shown in Figure 15.

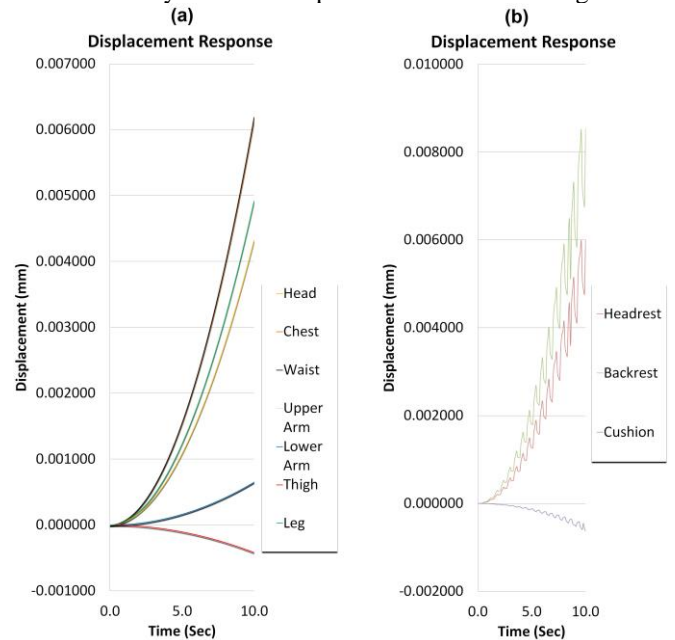


Figure 15: (a) Vertical displacements at the points of interest for human body
(b) Vertical displacements at the points of interest for car seat

The empirical co-relation between the mass, acceleration, displacement, damping, stiffness, time and frequency is shown in Equation 11.

$$\omega = \frac{1}{t} \text{Sin}^{-1} \left(\frac{m \times a + c \times v + k \times d}{F} \right) \quad (11)$$

- m = Mass
- a = Acceleration
- c = Damping coefficient
- v = Velocity
- k = Stiffness
- d = Displacement
- F = Force
- ω = Frequency
- t = Time

For multi-mass system, Equation 11 can be expressed in matrix format as shown in Equation 12.

$$[M]\{\ddot{X}\} + [C]\{\dot{X}\} + [K]\{X\} = \{f\} \quad (12)$$

Where,
[M] = Mass matrix

$[C]$ = Damping matrix
 $[K]$ = Stiffness matrix

$\{f\}$ = External force applied to the system.

Complex displacement function of multi-mass system can be denoted as a function of frequency ω and displacement X by

Fourier transformation of Equation 12 derives Equation 13, which can denote the complex displacement of multi-mass system as a function of frequency and displacement.

$$\{X(j\omega)\} = \left[[K] - \omega^2[M] + j\omega[C] \right]^{-1} \{F(j\omega)\} \quad (13)$$

Where,

$\{F(j\omega)\}$ $\{F(j\omega)\}$ = the complex Fourier transformation vector

of $\{f\}$ $\{f\}$

ω = Frequency

X = Displacement

Implementing the formulations of Equation 11, Equation 12 and Equation 13, the frequencies at all the designated points on the human body and car seat have been extracted and graphically plotted in Figure 16.

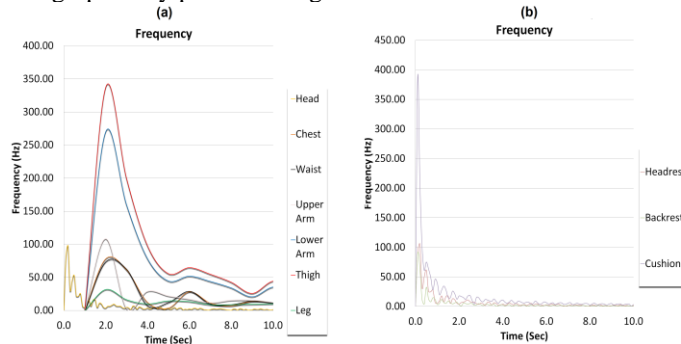


Figure 16: (a) Frequencies of human body portions (b) Frequencies of car seat components

The average and root mean square (RMS) frequencies of the human body and car seat portions have been calculated from the frequency plots and recorded in TABLE I.

TABLE I: Average and RMS frequencies of human segments.

Human segment	Average frequency (Hz)	RMS frequency (Hz)
Human: Head	7.10	15.85
Human: Chest	4.13	10.89
Human: Waist	4.18	10.69
Human: Upper Arm	4.01	12.06
Human: Lower Arm	12.92	34.45
Human: Thigh	16.13	43.03
Human: Leg	3.20	5.49
Seat: Headrest	7.91	17.64
Seat: Backrest	4.61	12.24
Seat: Cushion	18.00	48.47

IV. VALIDATION AND DISCUSSION

To validate the vertical accelerations obtained from this simulation technique, testing data have been gathered from an on-road non-racer type of car. A standard hatchback car with a male human driver of 78 kg mass was maintained to pick speed up to 30-35 miles/ hour from the static condition. There was no visible sign of irregular road terrain and the testing data had been recorded for 60 seconds.

Vibration measurement system NI 9234 module with CompactDAQ chassis and transducer Dytran 3055 had been utilized for reading out the vibration data at different points. A standard laptop with “m+p analyzer” software tool had been used for signal processing. Plots for vertical acceleration with respect to time and power spectrum density with respect to frequency had been logged. Arranged test set up and a sample of raw vibration data received for the thigh portion of human driver are displayed in Figure 17 and Figure 18, respectively.

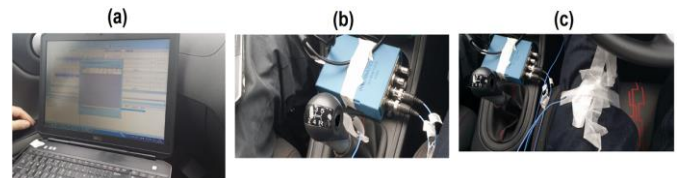


Figure 17: Test set up (a) Standard laptop with the signal processing tool “m+p Analyzer” (b) NI 9234 module for measurement (c) Dytran 3055 sensor mounted on human driver thigh

The raw testing data had been collected for a duration of initial 60 seconds. Later, the testing data were curtailed to initial 10 seconds to match to the span of simulation running time and filtered in .XLS format.

The vertical accelerations obtained from the simulation results and the corresponding vertical accelerations gathered from the testing data have been merged together though plots for convenient comparison purpose. Figure 19, Figure 20, Figure 21, Figure 22, Figure 23, Figure 24, Figure 25, Figure 26, Figure 27 and Figure 28 are showing the comprehensive contrasts between the simulation output and testing data in terms of vertical acceleration for all the segments of human body and car seat.

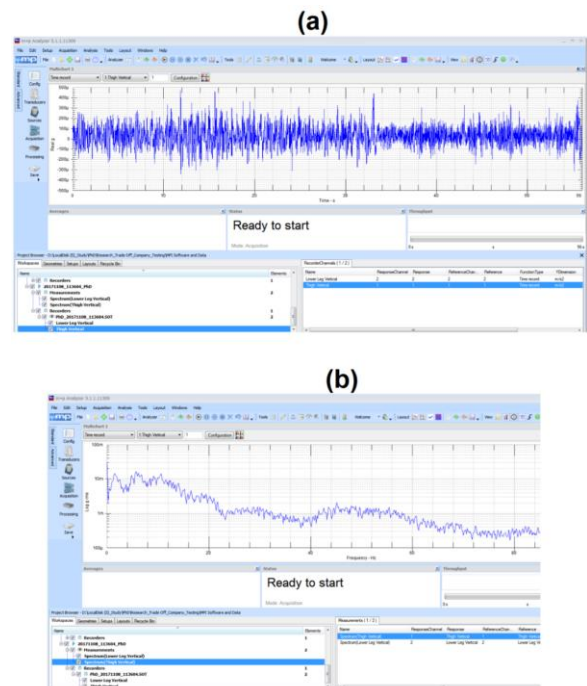


Figure 18: Raw vibration test data for human driver thigh (a) Acceleration vs time (b) Power spectrum density vs frequency

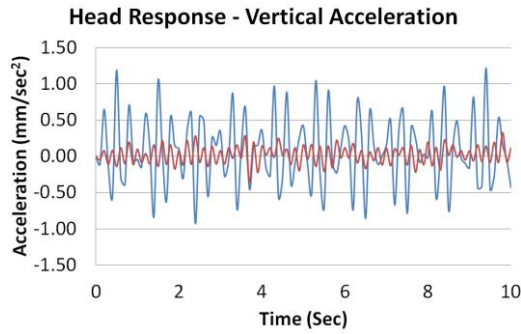


Figure 19: Vertical accelerations of human head from simulation (blue) and testing (red)

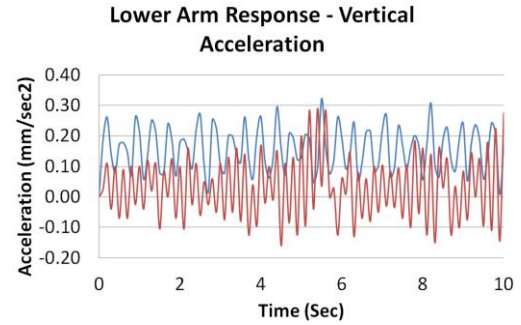


Figure 23: Vertical accelerations of human lower arm from simulation (blue) and testing (red)

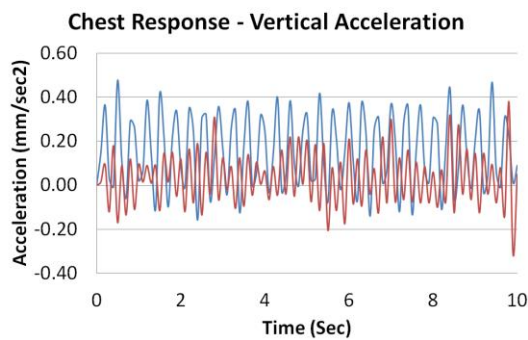


Figure 20: Vertical accelerations of human chest from simulation (blue) and testing (red)

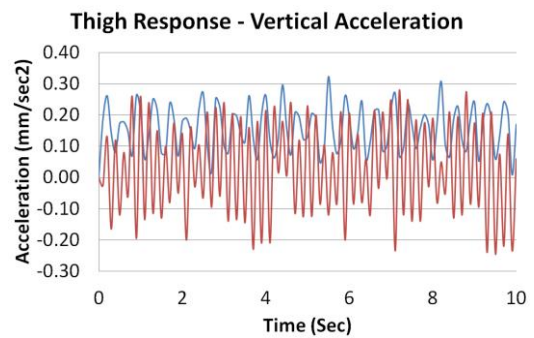


Figure 24: Vertical accelerations of human thigh from simulation (blue) and testing (red)

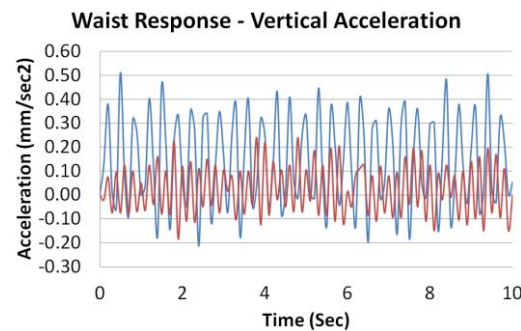


Figure 21: Vertical accelerations of human waist from simulation (blue) and testing (red)

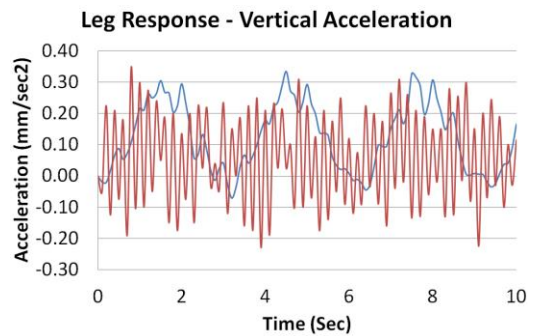


Figure 25: Vertical accelerations of human leg from simulation (blue) and testing (red)

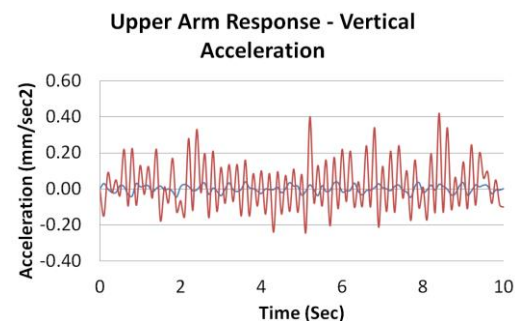


Figure 22: Vertical accelerations of human upper arm from simulation (blue) and testing (red)

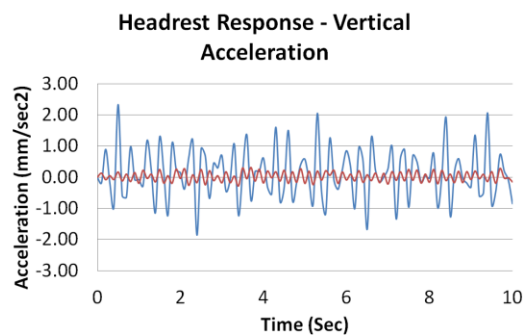


Figure 26: Vertical accelerations of seat headrest from simulation (blue) and testing (red)

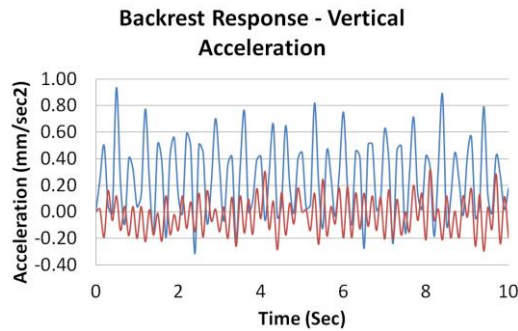


Figure 27: Vertical accelerations of seat backrest from simulation (blue) and testing (red)

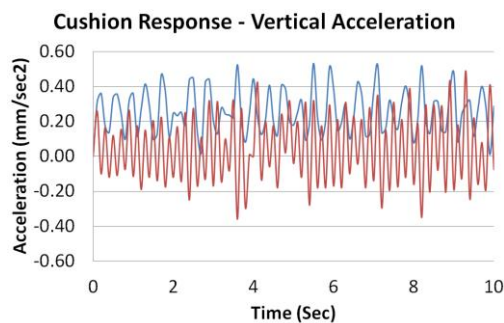


Figure 28: Vertical accelerations of seat cushion from simulation (blue) and testing (red)

From the comparison graphs, it is observed that the acceleration values from the simulation are more conservative than those of received from the testing. Graphs in Figure 20, Figure 22, Figure 23, Figure 27 and Figure 28 are showing the comparative data for the head, waist, upper arm, headrest and backrest, respectively, which indicate that the upper and lower limits of the testing data are falling well below the respective limits of the simulation results. Graphs in Figure 21, Figure 24, Figure 25 and Figure 28 are showing the comparisons of the vertical accelerations for the chest, lower arm, thigh and cushion, respectively, where the upper limits of the testing data are below the corresponding limits of the simulation results, but the lower limits of the testing data are exceeding the respective limits of simulation results. Graph in the Figure 26 is showing the comparison data of the leg, where both the upper and lower limits of the testing data are higher than the respective limits of the simulation results. If the absolute maximum magnitudes of all the plots are examined, then almost all the peak acceleration values from the testing data are lower than those from the simulation results.

To validate the frequency values obtained from this simulation work, past references in the similar fields have been consulted. In this simulation study, the average frequencies for the head, chest, waist, upper arm, lower arm, thigh, leg, headrest, backrest and cushion are obtained as 7.10 Hz, 4.13 Hz, 4.18 Hz, 4.01 Hz, 12.92 Hz, 16.13 Hz, 3.20 Hz, 7.91 Hz, 4.61 Hz and 18.00 Hz, respectively. Earlier biodynamic investigation on the human body [23] concluded that the range of resonating frequencies inside the human body under the effect of vertical vibration to be in between 0.5 Hz and 20 Hz. Similar kind of study on the human organs [46] evaluated the maximum natural frequencies for head, jaw,

eyes, chest, upper limb, stomach, bladder, pelvis, muscles and liver as 5 Hz, 8 Hz, 90 Hz, 9 Hz, 3 Hz, 10 Hz, 18 Hz, 9 Hz, 20 Hz and 4 Hz, respectively.

The assembled human body and the car seat configuration is a very complex system, where numerous parameters are involved and each of these parameters has got the ability to manipulate the system behaviour on its own. Study on vibration transmission in between the car seat and human body [47] utilized standard and rigid car seats and found that the vertical excitation would have great influence on the vertical vibration inside the human body and car seat. That study explored further the frequency values, which were found to be varying from one human body to other. The possible reasons for those variations were addressed as changes in the contact surface area and sitting posture. Similar kinds of research works on the human body and car seat [48], [49], [50] detailed the influence of the human posture on the vertical vibration transmission. Study on the vibration analysis of the car seat [48] reported that the resonance frequency would become higher for a more backward inclined car seat. Assessment of acceleration transmission from the seat to the human lumbar spine [51] found the natural frequencies to be in the range of 4 Hz to 5 Hz. Work on car seat to human head transmissibility [50] found the natural frequency value as 5 Hz. Acceleration transmission from seat to human trunk and associated mode shapes were inspected [49], [52] and the first two natural frequencies for the whole body were found to be 5 Hz and 8 Hz- 9 Hz. Resonating behaviour of the human body under the effect of vertical vibration [47] evaluated the natural frequency for the standard car seat as 5 Hz. International standard ISO 5892 (2001) defined the natural frequency as 5 Hz for the human sitting on a car seat without the backrest. International standards on biodynamics and ergonomics ISO/TC 159/SC 1, ISO/TC 159/SC 3 and ISO/TC 159/SC 4 recommend that the frequency of any human segment must not exceed the limit of 20 Hz while designing the human interfacing system.

The frequencies for the segments of the human body and car seat received from the current finite element based simulation study, are below the limit of 20 Hz. Hence, this unique simulation technique is successful in predicting the frequencies of the various portions of the human body and car seat. This methodology can be implemented to judge the health, comfort and safety levels of the seated human inside a moving car, regardless of the justified amounts of mismatches between the simulation results and testing data.

V. CONCLUSIONS AND SCOPES OF FURTHER DEVELOPMENT

In this research paper, a unique finite element based simulation technique has been proposed to predict the final levels of vibration at various locations of human body and seat inside a moving car. From the results of this research work, the following conclusions can be drawn:

A. This unique simulation technique can be implemented to anticipate the frequency levels at different segments of the human body and car seat. Inside the simulation environment, a lot of parameters have been incorporated,

namely; shape specific three dimensional stiffness values, damping parameters, Young’s moduli of the human body segments, boundary conditions, loading scenario, contact mechanism and analysis steps. In contrast, the testing data are greatly dependent on the instruments and signal processing systems. For explanation purpose, a simple spring-damper-mass system representing human pelvis and seat has been shown in Figure 29.

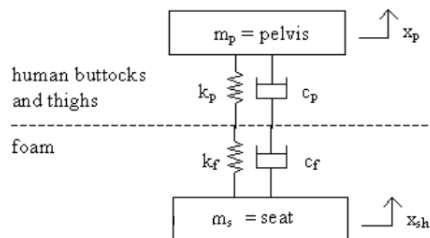


Figure 29: Spring-damper-mass system representing human and car seat

For any amount of vibration input to the seat, the resulting vibration at the human pelvis is a function of the frequency domain defined by the Laplace transform. The signal transfer function of the system for vibration transmission is presented in Equation 14.

$$H(s) = \frac{C_p \cdot s + K_p}{m_p \cdot s^2 + C_p \cdot s + K_p} \quad (14)$$

C_p = Total damping value

K_p = Total stiffness value

m_p = Mass of the human pelvis

s = Laplace domain transformation function

Equation 14 emphasizes that small alterations in the values of mass, damping and stiffness can tune the transfer function resulting the final vibration output to be changed. Hence, the mismatches between the simulation results and testing data are unavoidable. As the results from this unique simulation methodology are more conservative compared to the testing data, this simulation set up can be used for optimizing the health, comfort and safety levels of the car seated human body.

B. Human body segments can be represented through ellipsoids to calculate the shape specific three dimensional stiffness parameters for the human portions. The stiffness data evaluated in this research work, have the higher degrees of practicality than the stiffness parameters collected from standard database.

C. Average frequencies of the human body and car seat segments received from this unique simulation technique are below the permissible limit of 20 Hz, though the obtained peak frequency magnitudes are falling outside the allowable frequency ranges for the human organs. More detailed investigations on the simulation parameters are necessary to lower the peak frequency levels.

Enormous opportunities are there to improve this emerging simulation methodology further. Firstly, a longer span of simulation running time will help to obtain more

comprehensive acceleration and frequency plots. It is observed from the simulation outcomes that the frequency magnitudes are getting stabilized and lowered over the time. Therefore, longer simulation operating time will inevitably display lower ranges of frequencies for the segments of human driver and car seat. Secondly, each of the human segments can be split into more numbers of ellipsoids to form the physical anatomy of the human body. Three dimensional stiffness data for each of the ellipsoidal elements can be calculated, which will eventually provide more precise stiffness parameters for all the portions of the human body. Thirdly, viscoelastic properties can be assigned to the seat foam material besides the hyper-elastic properties. The frequency curves received from the simulation are getting steady over time, which indicates that the assigned stiffness values, damping coefficients and hyper-elastic material properties are behaving flawless inside the simulation environment. Incorporation of viscoelastic coefficients for the time dependent shear modulus function will yield more convincing results from the simulation. Lastly, in the present simulation study, only the vertical vibration has been assessed at different segments of the human body and car seat. To provide a more comprehensive solution, it will be beneficial to consider the fore-aft and sidewise vibrations.

VI. CONFLICT OF INTEREST

The outlined unique simulation technique presented in this research paper has no conflict of interest.

VII. ACKNOWLEDGEMENTS

Results from the simulation have been validated with the testing data provided by “m+p International”. Authors of this research paper are indebted to “m+p International” for all their helps and supports.

REFERENCES

- [1] A. Hellman, “Simulation of complete vehicle dynamics using FE code Abaqus”, *MSc Thesis- Luleå University of Technology*, pp. 19-31, 2008.
- [2] H. Y. Choi, M. Han, A. Hirao and H. Matsuoka, “Virtual Occupant Model for Riding Comfort Simulation”, *Proceedings of the 12th International Modelica Conference*, pp. 27-34, 2017.
- [3] K. Li, L. Zheng, S. Tashman and X. Zhang, “The inaccuracy of surface-measured model-derived tibiofemoral kinematics”, *Journal of Biomechanics*, vol. 45, no. 15, pp. 2719-2723, 2012.
- [4] C. Liu, Y. Qiu and M. J. Griffin, “A finite-element model of the vertical in-line and fore-and-aft cross-axis apparent mass and transmissibility of the human body sitting on a rigid seat and exposed to vertical vibration”, *In: Proceedings of the 47th UK conference on the human response to vibration*, pp. 17-19, 2012.
- [5] T. Kondo and Y. Ito, “Predicting ride comfort on seat using explicit FEM code”, *SAE Conference 2002, SAE no 2002-01-0779*, 2002.
- [6] P. Williamson, “Aspects of Simulation of Automobile Seating Using LS-Dyna 3D”, *Bamberg: LS-DYNA Anwenderforum*, pp. 53-60, 2005.
- [7] Y. Qiu and M. J. Griffin, “Transmission of fore-aft vibration to a car seat using field tests and laboratory simulation”, *Journal of Sound and Vibration*, vol. 264, no. 1, pp. 135–155, 2003.
- [8] R. J. Marshall, P.F. Altamore and D. Hartley, “Dynamic analysis of crew seats and cockpit interiors”, *SAE Conference 2000, SAE no 2000-01-1674*, 2000.
- [9] I. Mircheski, T. Kandikjan and S. Sidorenko, “Comfort analysis of vehicle driver’s seat through simulation of the sitting process”, *Analiza udobnosti vozačeva sjedala simulacijom postupka sjedanja*, vol. 21, no. 2, pp. 291-298, 2014.

- [10] R. Haan, "FE model of a car seat", *Netherlands Organisation for Applied Scientific Research*, pp. 9-12, 2002.
- [11] J. Zhang, N. Kikuchi, V. Li, A. Yee and G. Nusholtz, "Constitutive Modeling of Polymeric Foam Material Subjected to Dynamic Crash Loading". *International Journal of Impact Engineering*, vol. 21, no. 5, pp. 734-743, 1998.
- [12] S. Plagenhoef, F. G. Evans and T. Abdelnour, "Anatomical data for analyzing human motion", *Research Quarterly for Exercise and Sport*, vol. 54, pp. 169-178, 1983.
- [13] P. Leva, "Adjustments to Zatsiorsky-Seluyanov's Segment Inertia Parameters", *Journal of Biomechanics*, vol. 29, no. 9, pp. 1223-1230, 1996.
- [14] J. Majumder, J. "Anthropometric dimensions among Indian males — A principal component analysis", *Euras J Anthropol*, vol. 5, no. 2, pp. 54–62, 2014.
- [15] P. Ashby, "Ergonomics handbook 1: Human factors design data: Body size and strength. Pretoria: Tute Publication", 1975.
- [16] H. Bansal, "Mathematical validation of eigen values and eigen vectors of different human body segments in sitting posture", *MEng. Thesis, Thapar University*, 2013.
- [17] D. Hyun, S. Yoon, M. Kim and B. Juttler, "Modeling and Deformation of Arms and Legs Based on Ellipsoidal Sweeping", *Proceedings of the 11th Pacific Conference on Computer Graphics and Applications*, 2003.
- [18] Y. Zhang, W. Zhong, H. Zhu, Y. Chen, L. Xu and J. Zhu, "Establishing the 3-D finite element solid model of femurs in partial by volume rendering", *International Journal of Surgery*, vol. 11, pp. 930-934, 2013.
- [19] E. C. Wildman, "Foundations of the Human Body. Advanced human nutrition, 1st ed", 2000.
- [20] L. A. Spyrou and N. Aravas, "Muscle and Tendon Tissues: Constitutive Modeling and Computational Issues", *Journal of Applied Mechanics*, vol. 78, pp. 1-10, 2011.
- [21] E. J. Chen, J. Novakofski, W. K. Jenkins and W. D. O'Brien, "Young's Modulus Measurements of Soft Tissues with Application to Elasticity Imaging", *IEEE transactions on ultrasonics, ferroelectrics, and frequency control*, vol. 43, no. 1, pp. 191-194, 1996.
- [22] R. Muksian and C. D. Nash, "A model for the response of seated humans to sinusoidal displacements of the seat", *Journal of Biomechanics*, vol. 7, no. 3, pp. 209-215, 1974.
- [23] G. Zengkang, J. Andrew, A. J. Hillis and J. Darling, "Development of a Biodynamic Model of a Seated Human Body Exposed to Low Frequency Whole-body Vibration", *11th International Conference on Vibration ProblemsAt: Lisbon, Portugal*, 2013.
- [24] G. B. Kamalakar and A. C. Mitra, "Development and Analysis of Human Hand-Arm System Model for Anti-Vibration Isolators", *Materialstoday*, vol. 5, no. 2, pp. 3943-3952, 2017.
- [25] F. Lacquaniti, F. Licata and J. F. Soechting, (1982). "The mechanical behavior of the human forearm in response to transient perturbations", *Journal of Biological Cybernetics*, vol. 44, no. 1, pp. 35-46, 1982.
- [26] G. L. Gottlieb, G. C. Agarwal and R. Penn, "Sinusoidal oscillation of the ankle as a means of evaluating the spastic patient", *Journal of Neurol Neurosurg Psychiatry*, vol. 41, no. 1, pp. 32-39, 1978.
- [27] C. C. Gordon, T. Churchill, C. E. Clauser et al., "1988anthropometric survev of U.S. Army personnel: Methods and summary statistics, Final report (NATICWR- 891027) Natick", MA: *U.S. Army Natick Research, Development and Engineering Center*, 1989.
- [28] E. Grandjean, "Sitting posture of car drivers from the point of view of ergonomics, In D.J. Osborne and J.A. Levis (eds.), *Human Factors in Transport Research*", *User Factors: Comfort, the Environment and Behaviour*, New York: Academic Press, vol. 2, pp. 205-213, 1980.
- [29] J. J. Keegan, "The medical problem of lumbar spine flattening in automobile seats", *SAE Technical Paper 838A*. New York, NY: *Society of Automotive Engineers, Inc*, 1964.
- [30] M. Gruzjic, W. C. Bell, G. Arakere and I. Haque, "Finite element analysis of the effect of up-armouring on the off-road braking and sharp-turn performance of a high-mobility multi-purpose wheeled vehicle", *Proceedings of The Institution of Mechanical Engineers Part D-journal of Automobile Engineering - PROC INST MECH ENG D-J AUTO*. 10.1243/09544070JAUTO1187, vol. 223, pp. 1419-1434., 2009.
- [31] R. W. Ogden, "Large deformation isotropic elasticity – On the correlation of theoryand experiment for incompressible rubberlike solids", *InProceedings of the RoyalSociety of London Series A*, 1972, 326, pp. 565–584, 1972.
- [32] N. J. Mills, "Polymer Foams Handbook: Engineering and Biomechanics Applications and Design Guide", *Butterworth-Heinemann*, 2007.
- [33] M. Schrodt, G. Benderoth, A. Kuhhorn and G. Silber, "Hyperelastic Description of Polymer Soft Foams at Finite Deformations", *Technische Mechanik*, vol. 25, pp. 162-173, 2005.
- [34] U. Jarfelt and O. Ramnäs "Thermal conductivity of polyurethane foam Best performance", *In Proceedings of the 10th International Symposium on District Heating and Cooling, Hannover, Germany, 3–5 Sep*, pp. 1–12, 2006.
- [35] H. I. Y. Yousif, "Auxetic Polyurethane Foam (Fabrication, Properties and Applications)", *MSc Thesis, Helwan University*, 2012.
- [36] A. Milivojevich, G. R. Blair, J. G. Pageau, and J. D. van Heumen, "Automotive seating comfort; Defining comfort properties in Polyurethane Foam", *SAE*, 01-0587, pp. 1-10, 1999.
- [37] M. L. Ju, H. Jmal, R. Dupuis and E. Aubry, "Visco-hyperelastic constitutive model for modelling the quasi-static behavior of polyurethane foam in large deformation", *Polymer Engineering and Science, Wiley-Blackwell*, vol. 55, no. 8, pp.1795-1804, 2014.
- [38] R. S. Lakes and A. Lowe, A. "Negative Poisson's ratio foam as seat cushion material", *CellularPolymers*, vol. 19, pp.157-167, 2000.
- [39] A. Konosu, "Development of a Biofidelic Human Pelvic FE-Model with Several Modifications onto a Commercial Use Model for Lateral Loading Conditions", *SAE Technical Paper Series 2003-01-0163*, 2003.
- [40] D. Murakami, Y. Kitagawa, S. Kobayashi, R. Kent and J. Crandall, J, "Development and Validation of a Finite Element Model of a Vehicle", *SAE Technical Paper Series 2004-01-0325*, 2004.
- [41] G. Andreoni, G. C. Santambrogio, M. Rabuffetti and A. Pedotti, "Method for the analysis of posture and interface pressure of car drivers", *Applied Ergonomics*, vol. 33, pp.511-522, 2002.
- [42] A. Siefert, S. Pankoke and H. P. Wölfel, "Virtual optimisation of car passenger seats: Simulation of static and dynamic effects on drivers' seating comfort", *International Journal of Industrial Ergonomics*, vol. 38, pp.410–424, 2008.
- [43] G. Paul, J. Pendlebury and J. Miller, "The contribution of seat components to seat hardness and the interface between human occupant and a driver seat", *International Journal of Human Factors Modelling and Simulation (IJHFMS)*, vol. 3, no. 3/4, pp.378-397, 2012.
- [44] A. Mehar, S. Chandra and S. Velmurugan, "Speed and Acceleration Characteristics of Different Types of Vehicles on Multi-Lane Highways", *European Transport \ Trasporti Europei*, vol. 55, pp. 1-12, 2013.
- [45] R. M. Brooks, "Acceleration characteristics of vehicles in rural pennsylvania", *IJRRAS*, vol. 12, no. 3, pp. 449-453, 2012.
- [46] C. Cempel, "Applied vibroacoustic", *PWN, Warsaw*, 1989.
- [47] M. M. Verver, "Numerical tools for comfort analyses of automotive seating", *Eindhoven: Technische Universiteit Eindhoven*, pp. 7-70, 2004.
- [48] M. J. Griffin, "Handbook of human vibration. Academic press, London: Academic Press Limited", *ISBN 0-12-303040-4*, 1990.
- [49] S. Kitazaki and M. J. Griffin, "Resonance behaviour of the seated human body and effects of posture", *Journal of Biomechanics*, vol. 31, pp. 143-149, 1998.
- [50] C. L. Zimmermann and T. M. Cook, "Effects of vibration frequency and postural changes on human responses to seated whole-body vibration exposure", *Int Arch Occup Environ Health*, vol. 69, no.3, pp. 165-79, 1997.
- [51] M. M. Panjabi, G. B. J. Andersson, L. Jorneus, E. Hult and L. Mattsson, "In vivo measurement of spinal column vibrations", *Journal of Bone and Joint Surgery*, vol. 68, no. 5, pp. 695-702, 1986.
- [52] S. Kitazaki and M. J. Griffin, "A modal analysis of whole body vertical vibration, using a finite element model of the human body", *Journal of Sound and Vibration*, vol. 200, no. 1, pp. 83-103, 1997.